Carbohydrate Polymers 90 (2012) 1100–1105

Contents lists available at SciVerse ScienceDirect

Carbohydrate Polymers

journal homepage: www.elsevier.com/locate/carbpol

Application of a novel plasma-induced CD/MWCNT/iron oxide composite in zinc decontamination

Shitong Yang[a,*], Zhiqiang Guo[b], Guodong Sheng[a], Xiangke Wang[a]

[a] Key Laboratory of Novel Thin Film Solar Cells, Institute of Plasma Physics, Chinese Academy of Sciences, P.O. Box 1126, 230031 Hefei, PR China
[b] School of Resources and Environmental Engineering, Hefei University of Technology, 230009 Hefei, PR China

ARTICLE INFO

Article history:
Received 12 January 2012
Received in revised form 9 May 2012
Accepted 16 June 2012
Available online 23 June 2012

Keywords:
Plasma grafting
CD/MWCNT/iron oxide composite
Zn(II)
Magnetic separation
Reusability

ABSTRACT

Herein, β-cyclodextrin (β-CD) was grafted onto magnetic MWCNT/iron oxide particles by using low temperature plasma-induced technique to synthesize a novel nanocomposite. The prepared composite (denoted as CD/MWCNT/iron oxide) exhibited high magnetic property (saturation magnetization M_s = 37.8 emu/g) and good dispersion property in aqueous solution. Batch experiments were conducted to evaluate the application potential of CD/MWCNT/iron oxide in the decontamination of Zn(II) from aqueous solutions. The sorption amount of Zn(II) on CD/MWCNT/iron oxide was higher than that of Zn(II) on MWCNT/iron oxides and oxidized MWCNTs, indicating that the grafted β-CD could enhance the sorption capacity of CD/MWCNT/iron oxide composite toward Zn(II) by providing multiple hydroxyl functional groups. Due to its high magnetic, CD/MWCNT/iron oxide could be easily separated from aqueous solution with an external magnetic field. Regeneration studies suggested that CD/MWCNT/iron oxide can support long term use as a cost-effective material in sewage treatment with minimum replacement costs.

1. Introduction

Heavy metal pollution in soil and water systems has aroused worldwide concern during the last few decades due to its toxic impacts on ecological environment and human health (Jha, Upadhyay, Lee, & Kumar, 2008). The presence of heavy metal ions in drinking water above the permissible limit may directly or indirectly cause adverse health problems such as hepatitis, diarrhea, anemia, nephritic syndrome and the dysfunction of central nervous system (Al-Asheh & Banat, 2001; Mohan & Sreelakshmi, 2008). For the purpose of protecting ecosystem stability and public health, it is necessary to decrease the concentration of heavy metal ions to the permissible limits before their discharge to the environment. Conventional techniques for heavy metal pollution disposal include chemical precipitation, sorption, ion exchange, electrolysis froth flotation, membrane separation, liquid–liquid extraction and reverse osmosis (Bratskaya, Pestov, Yatluk, & Avramenko, 2009; Dąbrowski, Hubicki, Podkościelny, & Robens, 2004; Dermentzis, 2010; Molinari, Gallo, & Argurio, 2004; Yoon, Amy, Chung, Sohn, & Yoon, 2009). Among these methods, sorption has received increasing attention due to its multiple advantages such as convenient operation, high efficiency, low cost and wide adaptability.

The surface properties of adsorbents determine the performance of sewage disposal technology, including sorption capacity and post-treatment processes (i.e., separation and recovery), which correspondingly plays an important role in environmental contaminant disposal. Currently, ultracentrifugation and filtration are the main methods for separating adsorbents from aqueous phase. However, these two methods are unsatisfactory due to the fact that high speed centrifugation consumes vast electric energy and filtration is prone to filter blockages. In recent years, the application of magnetic adsorbents in wastewater disposal has received widespread attention due to its convenience and speediness in separation and recovery processes (Bayramoğlu & Arica, 2007; Hritcu, Humelnicu, Dodi, & Popa, 2012; Hu, Zhao, & Wang, 2011; Li et al., 2010; Zhou, Nie, Branford-White, He, & Zhu, 2009). After sorption equilibrium, the magnetic adsorbents can be easily separated and recovered with an external magnetic field. However, the further application of these materials is restricted due to their poor dispersibility and low sorption capacity. In view of this point, researchers are making great efforts to modify the surfaces of magnetic adsorbents with a variety of functionalized polymers such as gum arabic, ketoglutaric acid, calcium alginate, polyacrylic acid, chitosan, etc. Extensive studies have proved that the obtained magnetic composites exhibit good performance in the purification of both inorganic and organic contaminants (Badruddoza, Tay, Tan, Hidajat, & Uddin, 2011; Banerjee & Chen, 2007; Chen, Wang, & Nagatsu, 2009; Lim, Zheng, Zou, & Chen, 2009; Yan, Chang, Zheng, & Ma, 2012; Zhou et al., 2009).

* Corresponding author. Tel.: +86 551 5591368; fax: +86 551 5591310.
E-mail address: styang@ipp.ac.cn (S. Yang).

0144-8617/$ – see front matter © 2012 Elsevier Ltd. All rights reserved.
http://dx.doi.org/10.1016/j.carbpol.2012.06.049

Plasma-induced grafting technique is a novel method to introduce functional groups onto material surfaces without altering their bulk properties (Chevallier et al., 2001; Hu, Sheng, Ren, Chen, & Wang, 2011). In this study, a novel magnetic nanocomposite was synthesized by grafting β-CD onto the surfaces of MWCNT/iron oxides by using low temperature plasma-induced technique. The sorption properties of the prepared CD/MWCNT/iron oxide composite was investigated using Zn(II) as the target metal contaminant due to its extensive environmental impacts. Batch technique was adopted to investigate the removal of Zn(II) by CD/MWCNT/iron oxide under various solution chemistry conditions. Further investigations were conducted to evaluate the regeneration and reusability of CD/MWCNT/iron oxide. Finally, the sorption mechanism of Zn(II) on CD/MWCNT/iron oxide and the application potential of CD/MWCNT/iron oxide in sewage disposal were evaluated based on the obtained results.

2. Experimental

2.1. Materials

β-Cyclodextrin (β-CD) and zinc nitrate hexahydrate ($Zn(NO_3)_2{\cdot}6H_2O$) were purchased in analytical purity from Sinopharm Chemical Reagent Co. Ltd. (China). All other chemicals were purchased in analytical purity and used without further purification. All solutions were prepared with Milli-Q water under ambient conditions.

2.2. Synthesis and characterization of CD/MWCNT/iron oxides

MWCNTs were synthesized by chemical vapor deposition method of acetylene in hydrogen flow at 760 °C using Ni–Fe nanoparticles as catalysts. Oxidized MWCNTs were then prepared by oxidizing the pristine MWCNTs with 3 mol/L HNO_3 solution. MWCNT/iron oxide composite was prepared by using wet chemical coprecipitation process via the interactions between ferrous ions, ferric ions and oxidized MWCNTs. The preparation of CD/MWCNT/iron oxide composite composed of two successive processes, i.e., the surface activation of MWCNT/iron oxides by low temperature plasma and the grafting of β-CD on activated MWCNT/iron oxides (Hu et al., 2010). As expected, the grafted β-CD enhanced the dispersibility of MWCNT/iron oxides in aqueous solution.

The specific surface area of CD/MWCNT/iron oxide composite was measured to be 63.9 m^2/g by using N_2-BET method. The results of TGA analysis in previous study suggested that the content of β-CD grafted on MWCNT/iron oxides was 16.6 mg/g (Hu et al., 2010). The saturation magnetization (M_s) of CD/MWCNT/iron oxide was 37.8 emu/g, indicating that the prepared composite had a high magnetism. The XRD patterns of oxidized MWCNTs, MWCNT/iron oxides and CD/MWCNT/iron oxide composite were recorded on a MAC Science Co. M18XHF diffractometer using Cu Kα radiation (λ = 0.15406 nm). The measurements were carried out in the 2θ range of 10–70° with a scanning rate of 2°/min. FTIR spectra of CD/MWCNT/iron oxide before and after Zn(II) uptake were recorded with a FTIR spectrometer (Perkin Elmer spectrum 100, America) in the range of 4000–400 cm^{-1} using KBr pellets containing the prepared materials. The spectral resolution was set to 1 cm^{-1}, and 150 scans were collected for each spectrum.

2.3. Sorption experiments

All the batch experiments were carried out in polyethylene centrifuge tubes under ambient conditions. The CD/MWCNT/iron oxide suspension and $NaNO_3$ electrolyte solution were pre-equilibrated for 24 h, and then Zn(II) stock solution was added to achieve the desired concentrations of individual components. The pH of each test solution was adjusted to desired values by adding negligible volumes of 0.01 or 0.1 M HNO_3 or NaOH. The obtained suspensions were gently shaken on a rotating oscillator to attain sorption equilibrium, and then the solid and liquid phases were separated by using a permanent magnet. The concentration of Zn(II) in supernatant was analyzed by atomic absorption spectrophotometry. All experimental data were the average of duplicate determinations and the relative errors were ~5%. The sorption amount of Zn(II) on CD/MWCNT/iron oxide composite ($q_e = ((C_0 - C_e){\cdot}V/m)$) was derived from the initial Zn(II) concentration (C_0), the final Zn(II) concentration (C_e), the mass of CD/MWCNT/iron oxide (m) and the suspension volume (V).

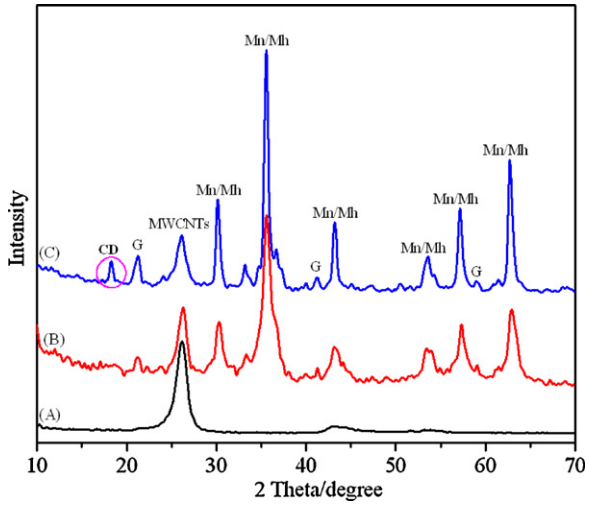

Fig. 1. XRD patterns of oxidized MWCNTs (A), MWCNT/iron oxides (B) and CD/MWCNT/iron oxide composite (C).

3. Results and discussion

3.1. Characterization of CD/MWCNT/iron oxide

Fig. 1 shows the XRD patterns of oxidized MWCNTs, MWCNT/iron oxides and CD/MWCNT/iron oxide composite, respectively. The characteristic diffraction peak of MWCNTs (i.e., $2\theta = 26.2°$) (curve A in Fig. 1) can be clearly seen in the patterns of the other two samples (curves B and C in Fig. 1), which suggests that the basic structure of MWCNTs is not destroyed during the chemical coprecipitation and plasma grafting processes (Hu et al., 2010). In the XRD pattern of MWCNT/iron oxides (curve B in Fig. 1), the appearances of six characteristic peaks at 30.21°, 35.56°, 43.24°, 53.62°, 57.22° and 62.95° reveal a cubic iron oxide phase, i.e., magnetite (JCPD No. 89-3854, denoted as Mn) and/or maghemite (JCPD No. 89-5892, denoted as Mh). Other peaks at 21.26°, 41.29° and 59.12° may be assigned to the main phases of goethite (denoted as G) (Oliveira et al., 2002). Furthermore, a new diffraction peak at 18.30° appears in the XRD pattern of CD/MWCNT/iron oxide composite (curve C in Fig. 1), which may arise from the introduction of β-CD on MWCNT/iron oxide surfaces (Song, Wang, Guo, & Bai, 2008). The grafted β-CD may have some influence on the surface properties of MWCNT/iron oxides and meanwhile provides plentiful oxygen-containing sites for Zn(II) binding.

To accurately understand the interaction between Zn(II) and CD/MWCNT/iron oxide, FTIR spectra were collected and analyzed to provide insight into the underlying sequestration mechanisms. Fig. 2 shows the FTIR spectra of CD/MWCNT/iron oxide composite before and after Zn(II) uptake. Although no obvious distinctions can be directly observed from the two spectra, FTIR spectrum of

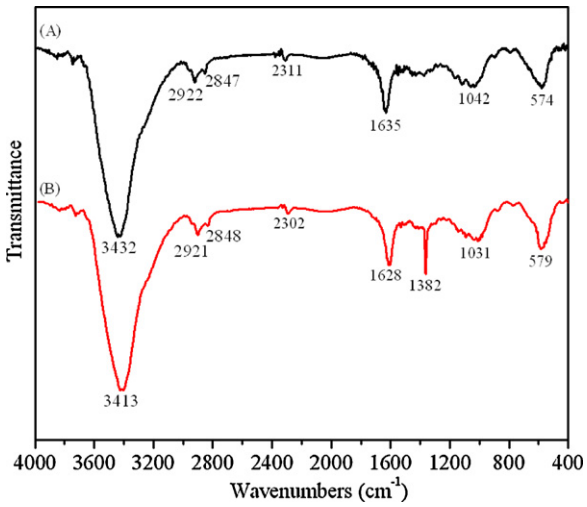

Fig. 2. FTIR spectra of CD/MWCNT/iron oxide composite before (A) and after Zn(II) uptake (B).

Zn(II)-sequestrated CD/MWCNT/iron oxide indeed shows that the peaks at 1042, 1635, 2311 and 3432 cm^{-1} have slightly shifted to 1031, 1628, 2302 and 3413 cm^{-1}, respectively. The shifting of these peaks suggests that their corresponding functional groups (mainly hydroxyl and carbonyl groups) may be directly involved in interaction with Zn(II) to form surface complexes. Since Zn(II) uptake on CD/MWCNT/iron oxide influences all the oxygenic chemical bonds, it is reasonable to deduce that the oxygen-containing functional groups would be the main surface sites for Zn(II) attachment (Badruddoza et al., 2011). In addition, a sharp band at ~1382 cm^{-1} appears in the FTIR spectrum of Zn(II)-sequestrated CD/MWCNT/iron oxide composite. This band can be assigned to the stretching vibration of NO_3^- ions, which are attached on CD/MWCNT/iron oxide surfaces to balance the electrical charges of adsorbed Zn(II) ions (Liu, Bai, & Ly, 2008; Takafuji, Ide, Ihara, & Xu, 2004). Furthermore, the peak of Fe–O has a slight shift from 574 to 579 cm^{-1}, suggesting that some Zn(II) ions are directly adsorbed on iron oxide surfaces (Lim, Zheng, Zou, & Chen, 2008).

3.2. Effect of contact time

Fig. 3A shows the kinetic data of Zn(II) sorption on CD/MWCNT/iron oxide at pH 6.5 and 303 K. The amount of adsorbed Zn(II) (mg/g) increases sharply during the first 2 h and thereafter it proceeds at a slow rate and finally attains equilibrium after 5 h. The initial rapid sorption may be attributed to the existence of plentiful binding sites on CD/MWCNT/iron oxide surfaces. The increase in concentration gradient tends to increase Zn(II) sorption rate at the initial stages. As contact time increases, the concentration gradient is gradually reduced due to the accumulation of Zn(II) on CD/MWCNT/iron oxide surfaces, leading to the decrease of sorption rate at the later stages. Overall, the sorption kinetics process becomes almost constant after a time period of 5 h. The fast sorption kinetics implies that CD/MWCNT/iron oxide may have good potentialities for continuous sewage disposal systems. Based on the above-mentioned kinetics data, the shaking time in the following experiments was fixed to 24 h to ensure complete equilibrium.

The surface properties and diffusion resistance of solid particles play an important role in the rate of sequestration as well as the overall transportation of metal ions. Specifically, the interaction processes before the sorption equilibrium may comprise the following steps (Ijagbemi, Baek, & Kim, 2009): (1) solute binds on the active sites via sorption, complexation or intra-particle precipitation processes; (2) solute transfers to the sorbent particle surface;

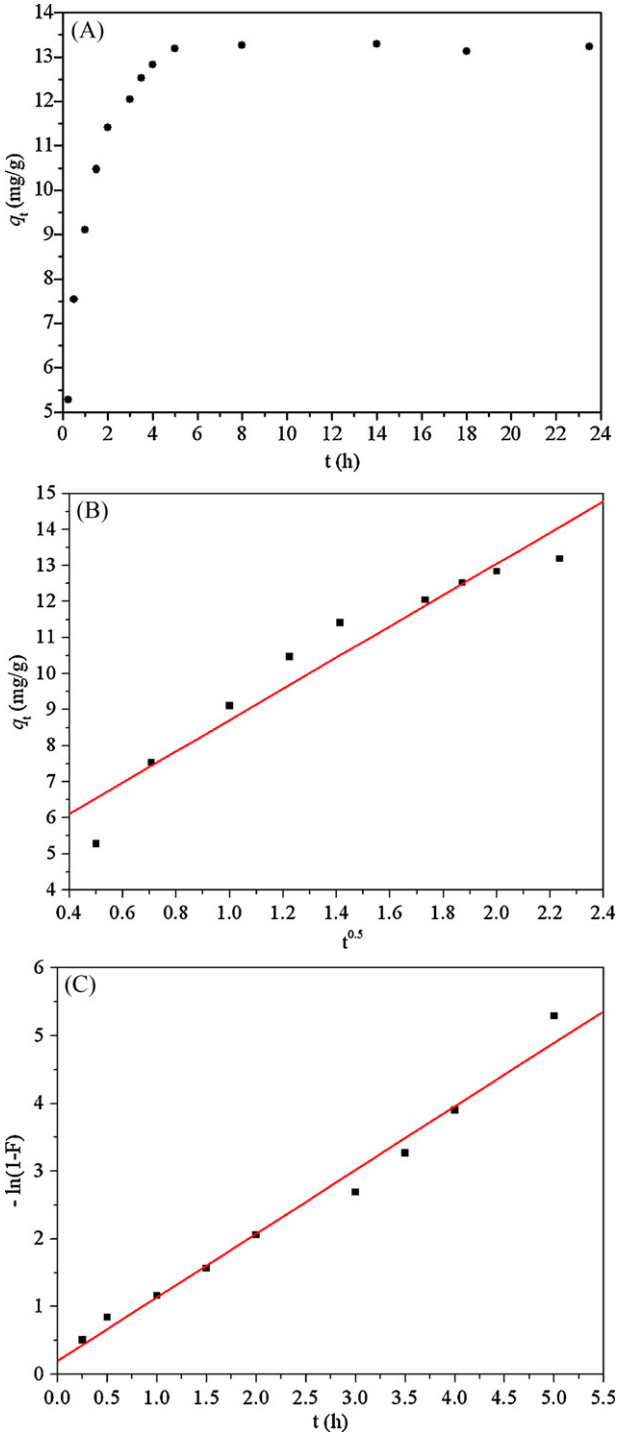

Fig. 3. Kinetic data of Zn(II) sorption on CD/MWCNT/iron oxide. pH 6.5, m/V = 0.4 g/L, $C_{Zn(II)initial}$ = 10 mg/L, T = 303 K, I = 0.01 M $NaNO_3$. (A) Plot of q_t vs. t; (B) intra-particle diffusion model fitting; (C) liquid film diffusion model fitting.

and (3) solute transfer from the particle surface to the intra-particle active sites. The first step is very rapid and can be considered negligible, while one of the (2) and (3) steps may be considered as the rate-limiting step for the sorption kinetic process. The (2) and (3) steps can be described by the liquid film diffusion model and intra-particle diffusion model, respectively. The intra-particle diffusion model can be expressed by the following equation (Wu, Zhao, & Yang, 2011):

$$q_t = k_i \cdot t^{0.5} \quad (1)$$

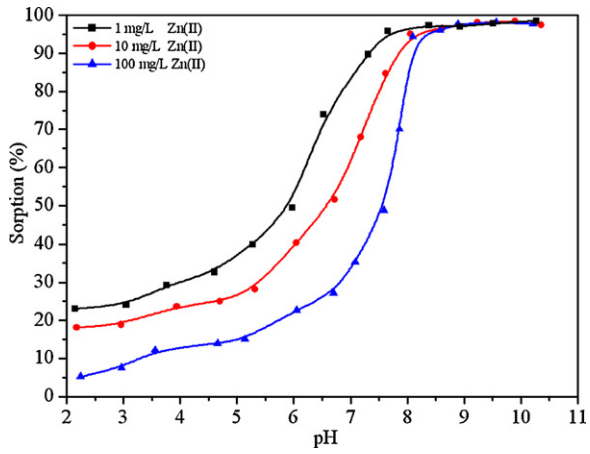

Fig. 4. Sorption of Zn(II) on CD/MWCNT/iron oxide as a function of initial Zn(II) concentrations. m/V = 0.4 g/L, T = 303 K, I = 0.01 M $NaNO_3$.

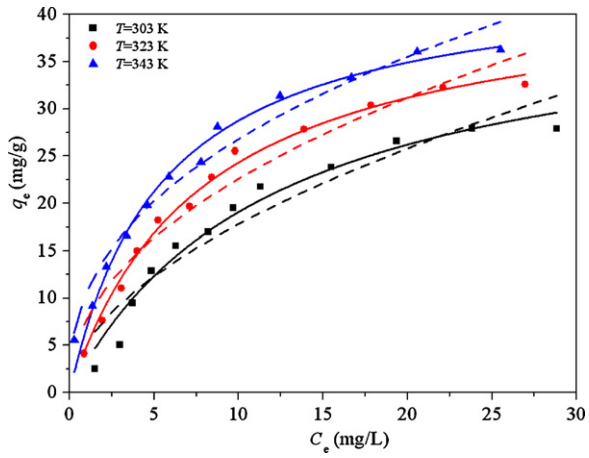

Fig. 5. Sorption isotherms and Langmuir, Freundlich models fitting for Zn(II) on CD/MWCNT/iron oxide. m/V = 0.4 g/L, pH 6.5, I = 0.01 M $NaNO_3$. Symbols represent experimental data, solid lines represent Langmuir model fitting and dash lines represent Freundlich model fitting.

where t (h) is the contact time, q_t (mg/g) is the amount of Zn(II) adsorbed on CD/MWCNT/iron oxide at time t, k_i (mg/g $h^{1/2}$) is the diffusion rate constant. Linear plot of q_t vs. $t^{0.5}$ is achieved according to Eq. (1) (Fig. 3B). The correlation coefficient (R^2) for the intra-particle diffusion model is 0.89. The intercept of the plot is 4.38 and the calculated k_i is 4.33 mg/g $h^{1/2}$. If the plot of q_t vs. $t^{0.5}$ presents as a straight line passing through the origin, the intra-particle diffusion may be the main driving force of the sorption kinetics (Gupta & Bhattacharyya, 2006). The value of correlation coefficient implies that the sorption kinetics might follow the intra-particle diffusion model; however, the nonzero intercept is not in line with the prediction of this model. In view of this point, the intra-particle diffusion is not the rate-determining step but it might have somewhat influence on the slow uptake process.

The liquid film diffusion model is governed by the equation (Gupta, Kumar, & Gaur, 2009):

$$\ln(1 - F) = -k_{fd}t \quad (2)$$

where F is the function attainment of equilibrium ($F = q_t/q_e$) and k_{fd} (h^{-1}) is the sorption rate constant. If the plot of $-\ln(1 - F)$ vs. t presents as a straight line with zero intercept, the sorption kinetics can be attributed to the liquid film diffusion process (Bhattacharyya & Gupta, 2008). However, the plot of $-\ln(1 - F)$ vs. t (Fig. 3C) gives a linear curve (R^2 = 0.98) with the intercept of 0.19 instead of zero, indicating that liquid film diffusion process may not be the singular rate-limiting step in the sorption process. It's worth noting that the correlation coefficient for liquid film diffusion model (R^2 = 0.98) is higher than that of intra-particle diffusion model (R^2 = 0.89), which suggests that the sorption kinetics of Zn(II) on CD/MWCNT/iron oxide is dominated by liquid film diffusion process accompanying with a certain contribution of intra-particle diffusion process.

3.3. Effect of initial Zn(II) concentrations

Fig. 4 shows Zn(II) sequestration on CD/MWCNT/iron oxide at three initial Zn(II) concentrations as a function of pH values. One can see that the sequestration curves show a typical "sorption edge", namely, the sequestration percentage increases from the minimum to the maximum over a range of more than three pH units. As expected, the sorption edge shifts to higher pH values at higher Zn(II) concentration. At pH < 8.0, the sorption of Zn(II) on CD/MWCNT/iron oxide increases with decreasing initial Zn(II) concentrations. In contrast, the sorption behavior seem to be independent of initial Zn(II) concentrations at pH > 8.0. Herein, it is necessary to verify whether the formation of $Zn(OH)_2$(s) precipitates contributes to the rapid increase of Zn(II) uptake by CD/MWCNT/iron oxide at pH < 8.0. Based on the activity coefficient value of Zn(II) in 0.01 mol/L $NaNO_3$ solution (i.e., 0.675), the actual chemical activity values for an initial Zn(II) concentrations of 1, 10 and 100 mg/L are calculated to be 0.675, 6.75 and 67.5 mg/L, respectively. Considering the solubility product constant of $Zn(OH)_2$(s) (i.e., $K_{sp} = 2.09 \times 10^{-16}$), one can deduce that Zn(II) ions begin to form hydroxide precipitates at pH 8.5, 8.1 and 7.5 for an actual Zn(II) chemical activity of 0.675, 6.75 and 67.5 mg/L (corresponding to initial Zn(II) concentrations of 1, 10 and 100 mg/L), respectively. However, one can see that more than 90% Zn(II) is sequestrated on CD/MWCNT/iron oxide at pH 8.0. Hence, for initial Zn(II) concentrations of 1 and 10 mg/L, the observed sequestration trend at pH < 8.0 may be attributed to surface complexation interaction rather than precipitation due to the low proportion of Zn(II) remained in solution (herein, <10%). In contrast, for initial Zn(II) concentration of 100 mg/L, the formation of $Zn(OH)_2$(s) precipitates doubtlessly plays a role in the dramatic increase of Zn(II) sequestration at pH < 8.0.

3.4. Sorption isotherms

Fig. 5 shows the sorption isotherms of Zn(II) on CD/MWCNT/iron oxide at three different temperatures (viz. 303, 323 and 343 K). It is clear that the sorption isotherm is the highest at T = 343 K and is the lowest at T = 303 K, which indicates that high temperature is beneficial for Zn(II) sorption. Several factors may account for the observed phenomenon: (1) the increase in temperature may increase the proportion and activity of Zn(II) ions in solution, the potential charge of CD/MWCNT/iron oxide and the corresponding affinity of CD/MWCNT/iron oxide toward Zn(II) ions (Partey, Norman, Ndur, & Nartey, 2008); (2) changes in CD/MWCNT/iron oxide pore sizes as well as the increase in the number of binding sites due to the breaking of some internal bonds are expected at higher temperatures (Yang et al., 2011); and (3) the diffusion rate of Zn(II) into CD/MWCNT/iron oxide pores may increase with increasing temperature (Genç-Fuhrman, Tjell, & McConchie, 2004).

For isotherm modeling, herein, Langmuir and Freundlich isotherm equations are conducted to simulate the sorption isotherms and to establish the relationship between the amount of Zn(II) adsorbed on CD/MWCNT/iron oxide and the concentration of Zn(II) remained in solution (Abdel-Halim & Al-Deyab, 2011;

Table 1
The parameters for Langmuir and Freundlich model fittings.

T (K)	Langmuir			Freundlich		
	q_{max} (mg/g)	b (L/mg)	R^2	K_F (mg^{1-n} L^n/g)	n	R^2
303	40.90	0.084	0.972	5.20	0.535	0.921
323	42.31	0.127	0.993	7.71	0.467	0.949
343	44.43	0.183	0.985	10.52	0.406	0.974

Gandhi, Kousalya, Viswanathan, & Meenakshi, 2011; Yang et al., 2010):

$$\text{Langmuir}: \quad q_e = \frac{bq_{max}C_e}{1 + bC_e} \tag{3}$$

$$\text{Freundlich}: \quad q_e = K_F C_e^n \tag{4}$$

where C_e is the equilibrium concentration of Zn(II) remained in the solution (mg/L); q_e is the amount of Zn(II) adsorbed on per weight unit of CD/MWCNT/iron oxide after equilibrium (mg/g); q_{max}, the maximum sorption capacity, is the amount of Zn(II) at complete monolayer coverage (mg/g), b (L/mg) is a constant that relates to the heat of sorption, K_F (mg^{1-n}·L^n/g) represents the sorption capacity when the equilibrium concentration of Zn(II) equals to 1, and n represents the degree of dependence of sorption with equilibrium concentration.

The fitting results of Langmuir and Freundlich models for Zn(II) sorption data are shown in Fig. 5. The relative parameters calculated from the two models are listed in Table 1. One can see from Fig. 5 that the two models fit the sorption isotherms well, which is also supported by the good correlation coefficients (all > 0.900) listed in Table 1. It can be concluded from the R^2 values that Langmuir model simulates the experimental data better than Freundlich model, indicating that the binding energy on the whole surface of CD/MWCNT/iron oxide is uniform. In other words, the whole surface has identical sorption activity and therefore the adsorbed Zn(II) ions do not interact with each other, and they are adsorbed by forming an almost complete monolayer coverage of the CD/MWCNT/iron oxide particles. This phenomenon also indicates that the sorption process is dominated by chemosorption (Zhou et al., 2009). Moreover, CD/MWCNT/iron oxide composite has a finite specific surface area and sorption capacity, thus the sorption data could be better simulated by Langmuir model rather than by Freundlich model, as an exponentially increasing sorption is assumed in the latter. A large value of b implies strong binding of Zn(II) on CD/MWCNT/iron oxide. The large K_F values of Freundlich model indicate that CD/MWCNT/iron oxide has a high sorption affinity toward Zn(II). The small n values imply that a nonlinear sorption occurs on CD/MWCNT/iron oxide surfaces.

3.5. Effect of grafted β-CD on Zn(II) uptake

To determine the specific contribution of grafted β-CD on Zn(II) uptake, we carefully compared the sorption amount of Zn(II) on oxidized MWCNTs, MWCNT/iron oxides and CD/MWCNT/iron oxide at pH 6.5. Despite the specific surface area of CD/MWCNT/iron oxide (63.9 m^2/g) is lower than that of MWCNT/iron oxides (88.5 m^2/g) and oxidized MWCNTs (197.0 m^2/g) (Hu et al., 2010), the sorption amount of Zn(II) on CD/MWCNT/iron oxide (13.1 mg/g) is higher than that on MWCNT/iron oxides (8.7 mg/g) and oxidized MWCNTs (10.2 mg/g). This phenomenon suggests that the grafted β-CD plays an important role in enhancing the sorption capacity of CD/MWCNT/iron oxide composite toward Zn(II). β-CD is a kind of oligosaccharide that consists of seven α-D-glucose units. Its characteristic truncated-cone structure contains an apolar cylindrical cavity with primary hydroxyl groups lying on the outside and secondary hydroxyl groups inside (Badruddoza et al., 2011). These hydroxyl groups can form strong complexes with Zn(II) and correspondingly enhance the sorption capacity of CD/MWCNT/iron oxide toward Zn(II).

3.6. Regeneration and reusability studies

From the economics standpoint, it is essential to use a cheap and high-efficiency material so as to minimize the cost of sewage disposal. In view of this point, the reusability of CD/MWCNT/iron oxide through many cycles of sorption/desorption experiments was investigated to evaluate the application potential of this material in the decontamination of real Zn(II)-bearing wastewater. Considering the loss of the CD/MWCNT/iron oxide during each cycle, the amount of CD/MWCNT/iron oxide and the volume of Zn(II) solution were adjusted to the comparable measurement. The sorption amount of Zn(II) on CD/MWCNT/iron oxide decreases slightly from 13.1 mg/g to 12.6 mg/g after six cycles. The excellent regeneration capacity suggests that CD/MWCNT/iron oxide can support long term use as a cost-effective material in sewage treatment with minimum replacement costs.

4. Conclusions

In this study, low temperature plasma-induced technology was adopted to synthesize a novel nanocomposite by grafting β-CD on MWCNT/iron oxide nanoparticles. The prepared CD/MWCNT/iron oxide nanocomposite was used in the decontamination of Zn(II) from aqueous solution. The sorption kinetics was dominated by liquid film diffusion process accompanying with a certain contribution of intra-particle diffusion process. The grafted β-CD enhanced the sorption capacity of CD/MWCNT/iron oxide toward Zn(II) by providing multiple hydroxyl binding sites. Reusability studies showed that CD/MWCNT/iron oxide still exhibited good sorption capacity toward Zn(II) after six cycles of sorption/desorption experiments. Besides, CD/MWCNT/iron oxide could be easily separated from the aqueous solution with an external magnetic field. Hence, this nanocomposite can be used as a cost-effective material for the decontamination of Zn(II) from wastewaters. More investigations are ongoing in our laboratory to further evaluate the application potential of CD/MWCNT/iron oxide in environmental pollution cleanup.

Acknowledgements

Financial supports from the National Natural Science Foundation of China (20971126; 21077107) and National Basic Research Program of China (2011CB933700) are acknowledged.

References

Abdel-Halim, E. S., & Al-Deyab, S. S. (2011). Removal of heavy metals from their aqueous solutions through adsorption onto natural polymers. *Carbohydrate Polymers*, *84*, 454–458.

Al-Asheh, S., & Banat, F. (2001). Adsorption of copper and zinc by oil shale. *Environmental Geology*, *40*, 693–698.

Badruddoza, A. Z. M., Tay, A. S. H., Tan, P. Y., Hidajat, K., & Uddin, M. S. (2011). Carboxymethyl-β-cyclodextrin conjugated magnetic nanoparticles as nano-adsorbents for removal of copper ions: Synthesis and adsorption studies. *Journal of Hazardous Materials*, *185*, 1177–1186.

Banerjee, S. S., & Chen, D. H. (2007). Fast removal of copper ions by gum arabic modified magnetic nano-adsorbent. *Journal of Hazardous Materials*, *147*, 792–799.

Bayramoğlu, G., & Arica, M. Y. (2007). Kinetics of mercury ions removal from synthetic aqueous solutions using by novel magnetic p(GMA-MMA-EGDMA) beads. *Journal of Hazardous Materials*, *144*, 449–457.

Bhattacharyya, K. G., & Gupta, S. S. (2008). Kaolinite and montmorillonite as adsorbents for Fe(III), Co(II) and Ni(II) in aqueous medium. *Applied Clay Science*, *41*, 1–9.

Bratskaya, S. Yu., Pestov, A. V., Yatluk, Yu. G., & Avramenko, V. A. (2009). Heavy metals removal by flocculation/precipitation using N-(2-carboxyethyl)chitosans. *Colloids and Surfaces A: Physicochemical and Engineering Aspects*, *339*, 140–144.

Chen, C. L., Wang, X. K., & Nagatsu, M. (2009). Europium adsorption on multiwall carbon nanotube/iron oxide magnetic composite in the presence of polyacrylic acid. *Environmental Science & Technology*, *43*, 2362–2367.

Chevallier, P., Castonguay, M., Turgeon, S., Dubrulle, N., Mantovani, D., McBreen, P. H., et al. (2001). Ammonia RF-plasma on PTFE surfaces: Chemical characterization of the species created on the surface by vapor-phase chemical derivatization. *The Journal of Physical Chemistry B*, *105*, 12490–12497.

Dąbrowski, A., Hubicki, Z., Podkościelny, P., & Robens, E. (2004). Selective removal of the heavy metal ions from waters and industrial wastewaters by ion-exchange method. *Chemosphere*, *56*, 91–106.

Dermentzis, K. (2010). Removal of nickel from electroplating rinse waters using electrostatic shielding electrodialysis/electrodeionization. *Journal of Hazardous Materials*, *173*, 647–652.

Gandhi, M. R., Kousalya, G. N., Viswanathan, N., & Meenakshi, S. (2011). Sorption behaviour of copper on chemically modified chitosan beads from aqueous solution. *Carbohydrate Polymers*, *83*, 1082–1087.

Genç-Fuhrman, H., Tjell, J. C., & McConchie, D. (2004). Adsorption of arsenic from water using activated neutralized red mud. *Environmental Science & Technology*, *38*, 2428–2434.

Gupta, S., Kumar, D., & Gaur, J. P. (2009). Kinetic and isotherm modeling of lead(II) sorption onto some waste plant materials. *Chemical Engineering Journal*, *148*, 226–233.

Gupta, S. S., & Bhattacharyya, K. G. (2006). Removal of Cd(II) from aqueous solution by kaolinite, montmorillonite and their poly(oxo zirconium) and tetrabutylammonium deriviates. *Journal of Hazardous Materials*, *128*, 247–257.

Hritcu, D., Humelnicu, D., Dodi, G., & Popa, M. I. (2012). Magnetic chitosan composite particles: Evaluation of thorium and uranyl ion adsorption from aqueous solutions. *Carbohydrate Polymers*, *87*, 1185–1191.

Hu, J., Shao, D. D., Chen, C. L., Sheng, G. D., Li, J. X., Wang, X. K., et al. (2010). Plasma induced grafting of cyclodextrin onto multiwall carbon nanotube/iron oxides for adsorbent application. *The Journal of Physical Chemistry B*, *114*, 6779–6785.

Hu, J., Sheng, G. D., Ren, X. M., Chen, C. L., & Wang, X. K. (2011). Removal of 1-naphthylamine from aqueous solution by β-cyclodextrin plasma grafted multiwall carbon nanotubes/iron oxides. *Journal of Hazardous Materials*, *185*, 463–471.

Hu, J., Zhao, D. L., & Wang, X. K. (2011). Removal of Pb(II) and Cu(II) from aqueous solution using multiwalled carbon nanotubes/iron oxide magnetic composites. *Water Science and Technology*, *63*, 917–923.

Ijagbemi, C. O., Baek, M. H., & Kim, D. S. (2009). Montmorillonite surface properties and sorption characteristics for heavy metal removal from aqueous solutions. *Journal of Hazardous Materials*, *166*, 538–546.

Jha, M. K., Upadhyay, R. R., Lee, J., & Kumar, V. (2008). Treatment of rayon waste effluent for the removal of Zn and Ca using Indion BSR resin. *Desalination*, *228*, 97–107.

Li, G. X., Du, Y. M., Tao, Y. Z., Deng, H. B., Luo, X. G., & Yang, J. H. (2010). Iron(II) cross-linked chitin-based gel beads: Preparation, magnetic property and adsorption of methyl orange. *Carbohydrate Polymers*, *82*, 706–713.

Lim, S. F., Zheng, Y. M., Zou, S. W., & Chen, J. P. (2008). Characterization of copper adsorption onto an alginate encapsulatedmagnetic sorbent by a combined FT-IR, XPS, and mathematical modeling study. *Environmental Science & Technology*, *42*, 2551–2556.

Lim, S. F., Zheng, Y. M., Zou, S. W., & Chen, J. P. (2009). Removal of copper by calcium alginate encapsulated magnetic sorbent. *Chemical Engineering Journal*, *152*, 509–513.

Liu, C., Bai, R., & Ly, Q. S. (2008). Selective removal of copper and lead ions by diethylenetriamine-functionalized adsorbent: Behaviors and mechanisms. *Water Research*, *42*, 1511–1522.

Mohan, S., & Sreelakshmi, G. (2008). Fixed bed column study for heavy metal removal using phosphate treated rice husk. *Journal of Hazardous Materials*, *153*, 75–82.

Molinari, R., Gallo, S., & Argurio, P. (2004). Metal ions removal from wastewater or washing water from contaminated soil by ultrafiltration-complexation. *Water Research*, *38*, 593–600.

Oliveira, L. C. A., Rios, R. V. R. A., Fabris, J. D., Garg, V., Sapag, K., & Lago, R. M. (2002). Activated carbon/iron oxide magnetic composites for the adsorption of contaminants in water. *Carbon*, *40*, 2177–2183.

Partey, F., Norman, D., Ndur, S., & Nartey, R. (2008). Arsenic sorption onto laterite iron concretions: Temperature effect. *Journal of Colloid and Interface Science*, *321*, 493–500.

Song, L. X., Wang, H. M., Guo, X. Q., & Bai, L. (2008). A comparative study on the binding behaviors of β-cyclodextrin and its two derivatives to four fanlike organic guests. *The Journal of Organic Chemistry*, *73*, 8305–8316.

Takafuji, M., Ide, S., Ihara, H., & Xu, Z. H. (2004). Preparation of poly(1-vinylimidazole)-grafted magnetic nanoparticles and their application for removal of metal ions. *Chemistry of Materials*, *16*, 1977–1983.

Wu, X. L., Zhao, D. L., & Yang, S. T. (2011). Impact of solution chemistry conditions on the sorption behavior of Cu(II) on Lin'an montmorillonite. *Desalination*, *269*, 84–91.

Yan, L., Chang, P. R., Zheng, P. W., & Ma, X. F. (2012). Characterization of magnetic guar gum-grafted carbon nanotubes and the adsorption of the dyes. *Carbohydrate Polymers*, *87*, 1919–1924.

Yang, S. T., Sheng, G. D., Tan, X. L., Hu, J., Du, J. Z., Montavon, G., et al. (2011). Determination of Ni(II) uptake mechanisms on mordenite surfaces: A combined macroscopic and microscopic approach. *Geochimica et Cosmochimica Acta*, *75*, 6520–6534.

Yang, S. T., Zhao, D. L., Zhang, H., Lu, S. S., Chen, L., & Yu, X. J. (2010). Impact of environmental conditions on the sorption behavior of Pb(II) in Na-bentonite suspensions. *Journal of Hazardous Materials*, *183*, 632–640.

Yoon, J., Amy, G., Chung, J., Sohn, J., & Yoon, Y. (2009). Removal of toxic ions (chromate, arsenate, and perchlorate) using reverse osmosis, nanofiltration, and ultrafiltration membranes. *Chemosphere*, *77*, 228–235.

Zhou, Y. T., Nie, H. L., Branford-White, C., He, Z. Y., & Zhu, L. M. (2009). Removal of Cu^{2+} from aqueous solution by chitosan-coated magnetic nanoparticles modified with α-ketoglutaric acid. *Journal of Colloid and Interface Science*, *330*, 29–37.